

Sample size effects on the large strain bursts in submicron aluminum pillars

Zhang-Jie Wang,¹ Qing-Jie Li,¹ Zhi-Wei Shan,^{1,a)} Ju Li,^{1,2,b)} Jun Sun,¹ and Evan Ma^{1,3,c)}

¹Center for Advancing Materials Performance from the Nanoscale (CAMP-Nano) and Hysitron Applied Research Center in China (HARCC), State Key Laboratory for Mechanical Behavior of Materials, Xi'an Jiaotong University, Xi'an 710049, People's Republic of China

²Department of Nuclear Science and Engineering and Department of Materials Science and Engineering, Massachusetts Institute of Technology, Cambridge, Massachusetts 02139, USA

³Department of Materials Science and Engineering, Johns Hopkins University, Baltimore, Maryland 21218, USA

(Received 16 October 2011; accepted 30 December 2011; published online 14 February 2012)

In situ transmission electron microscope compression testing of submicron Al pillars shows two sample size regimes with contrasting behavior underlying the large strain bursts. For small pillars, the bursts originate from explosive and highly correlated dislocation generation, characterized by very high collapse stresses and nearly dislocation-free post-collapse microstructure. For larger pillars, the bursts result from the reconstruction of jammed dislocation configurations, featuring relative low stress levels and retention of dislocation network after bursts. © 2012 American Institute of Physics. [doi:10.1063/1.3681582]

In the last several years, the sample size effects on the plasticity of metals have been widely investigated by compression tests of micro- and nano-sized pillars.^{1–11} It has been discovered that the plastic flow of submicron face-centered-cubic (fcc) single-crystal pillars can manifest instabilities generally characterized by pronounced strain bursts, besides the well-known tenet of “smaller is stronger.” For the strength trend, recent studies have attributed it to dislocation starvation² and surface nucleation¹² for pillars in the deep sub-micrometer size range, whereas for pillars with larger diameters, the single-arm dislocation source truncation hardening mechanism^{13,14} may be dominant. Comparatively speaking, the origin of the large strain bursts is less well understood. The analysis so far deals mostly with the magnitude and frequency of their occurrence.^{9,15–17} Through three-dimensional discrete dislocation dynamics (3D-DDD) simulations, Csikor *et al.*¹⁵ suggested that the bursts are due to long-range mutual interactions that make the destruction of jammed configurations in a collective, avalanche-like process: the dislocations liberated from jammed dislocation configurations fly around at high velocities to result in an instantaneously high strain rate. However, there has been no direct experimental evidence for this hypothesis. In addition, this unjamming mechanism cannot explain the large strain bursts leading to collapse of pillars with dislocation-free initial structure.^{18,19}

Here we use *in situ* compression of Al pillars inside a transmission electron microscope (TEM) to directly monitor the internal dislocation microstructural evolution accompanying the major strain bursts. We show that sample size strongly influences the burst behavior, in terms of the stress-strain evolution and the stress level at which the burst happens. There is in fact a sample size regime where dislocation jamming is absent *before* and *after* the burst, with a mechanism different from that depicted from previous work.¹⁵

Single-crystal Al nanopillars with diameters (D) from 80 nm to 1000 nm were fabricated using dual-beam focused-ion-beam (FIB). The starting Al piece had a thickness of 200 μm and a diameter of 3 mm. The Al slice was mechanically polished on both sides to a thickness of 50 μm . One side of the slice was then subjected to twin-jet polishing to obtain a thin region several micrometers in thickness, in a chemical solution of methanol with 5% perchloric acid. Inside the thin region, pillars with different diameters were FIB-fabricated. High-resolution TEM observation of the present Al pillars indicated that the surface amorphous layer is less than 1 nm thick. The *in situ* compression tests were carried out inside a JEM 2100 FEG TEM using a Hysitron PI95 TEM PicoIndenter in displacement-controlled mode due to its greater sensitivity to transient phenomena.²⁰ The corresponding dislocation microstructural evolution was recorded with a Gatan 830 (SC200) CCD camera. The one-to-one correlation between the mechanical stress-strain response and the dislocation configurations, before and after the burst transient, allows for the identification of the underlying mechanisms and sample size effects.

Large strain bursts were universally observed during the compression of our submicron sized Al pillars. However, depending on the sample size, the underlying physical mechanisms are different. For small pillars (with $D = 80$ to 300 nm, group A), the bursts originate from explosive and highly correlated dislocation generation, characterized by very high collapse stresses and nearly dislocation-free microstructure after the sample collapse. Figure 1 shows the $D = 165$ nm pillar as an example, representative of the group A pillars. Figure 1(a) is the engineering stress-strain curve. The evolution of force and displacement as a function of time is shown in Fig. 1(b). The single crystal pillar is loaded along the $[2\bar{2}0]$ direction, observed under $\langle 110 \rangle$ zone axis. FIB-introduced defects and pre-existing dislocations can be clearly seen in the bright-field image (Fig. 1(c)) and dark-field image (Fig. 1(d)). Well before the global collapse, the small stress drop, marked point 1 in the curves given in Figs. 1(a) and 1(b), is caused by the cleaning-up of pre-existing

^{a)}Electronic mail: zwshan@mail.xjtu.edu.cn.

^{b)}Electronic mail: liju@mit.edu.

^{c)}Electronic mail: ema@jhu.edu.

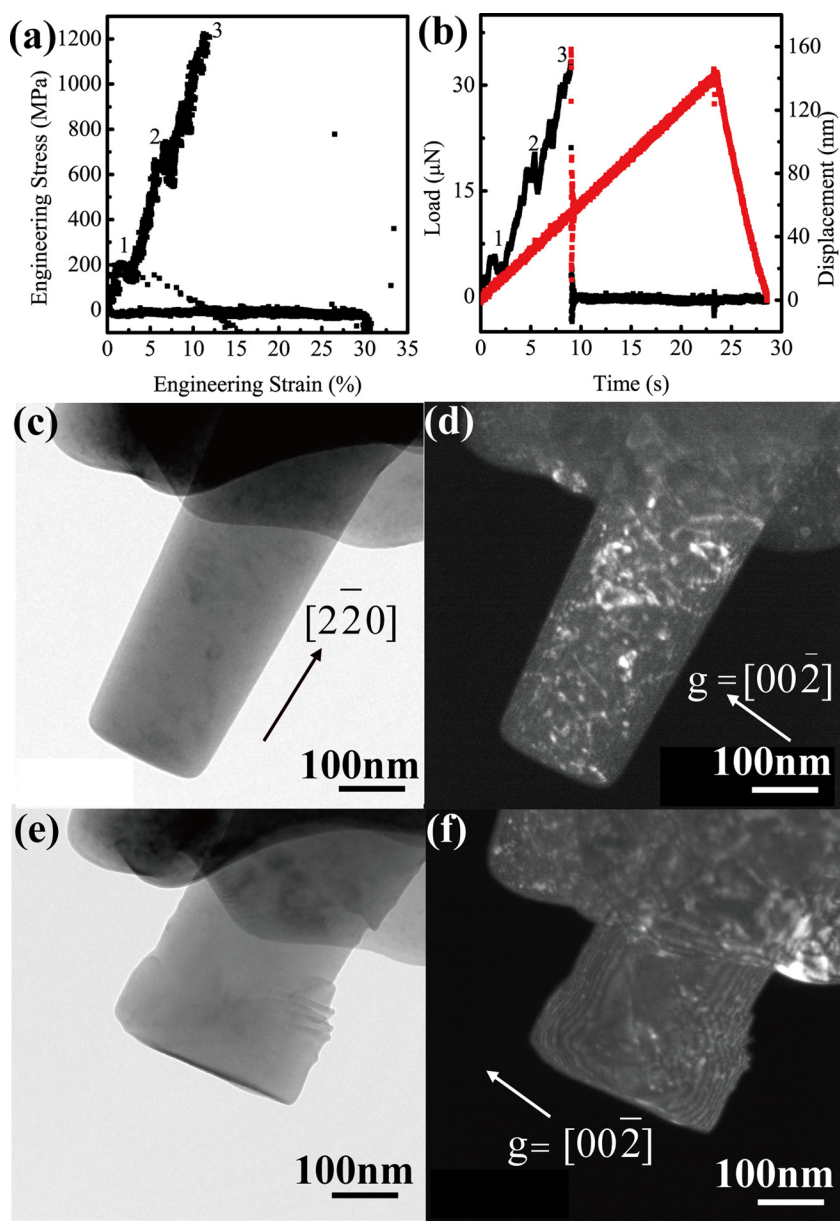


FIG. 1. (Color online) Snapshots of the microstructural evolution in Al nanopillar with $D = 165$ nm. (a) Engineering stress vs. engineering strain. (b) The load and displacement vs. time curves. (c) Bright-field image and (d) dark-field image of the pillar before compression. (e) Bright-field image and (f) dark-field image of the pillar after collapse ($\sim 20\%$ strain) (enhanced online) [URL: <http://dx.doi.org/10.1063/1.3681582.1>].

dislocations: they were driven out of the pillar, in a process known as mechanical annealing.²¹ At the second stress serration, marked point 2, new dislocations emerge from the contact interface between the pillar and the punch. But similar to the scenario at point 1, these dislocations escape immediately out of the pillar. Point 3 is where the global structural collapse occurred. The drastic strain burst in Fig. 2(a) is now observed to result in a major shape change within a small fraction of a second in movie S1.²⁴ The postmortem TEM observation under different tilting angle confirmed that the pillar was indeed almost dislocation free, as shown in Figs. 1(e) and 1(f). It appears that all the dislocation activities responsible for the dramatic shape change happened instantly, bursting in a sample after mechanical annealing and leaving no traces behind for postmortem observation. This scenario is in contrast to the avalanche from the stored and jammed dislocations depicted in computer simulations,^{15,22} which happened only in group B pillars (with $D = 300$ to 1000 nm).

The dislocation evolution in larger pillars (group B) is presented in Fig. 2, using the $D = 430$ nm pillar as an exam-

ple, imaged under approximately the two-beam condition (with a strong diffraction $\mathbf{g} = [1\bar{1}\bar{3}]$). Its engineering stress-strain curve is shown in Fig. 2(a). Before compression, a high density of pre-existing dislocations is observed in Fig. 2(b). During compression, instead of reaching a mechanically annealed state as in group A pillars, the dislocations were continuously operating during the entire deformation process, as shown in movie S2.²⁴ For the first several smaller strain bursts, the dislocation density was reduced a bit or maintained at almost the same level. Initially the dislocations self-organized to form a jammed configuration, which was destructed somewhat upon further increasing of the external load and reconstructed again, causing these stress serrations (see Fig. 2(a) and movie S2 (Ref. 24)). For example, at the larger strain burst ($\sim 3\%$) marked by point 1, the dislocation density increased a lot. This suggests dislocation multiplication and storage. Many of the generated dislocations could not escape and formed new junctions and tangles as new sources. Therefore, the next burst can occur at a lower stress, marked as point 2 in Fig. 2(a). Here, the observations are

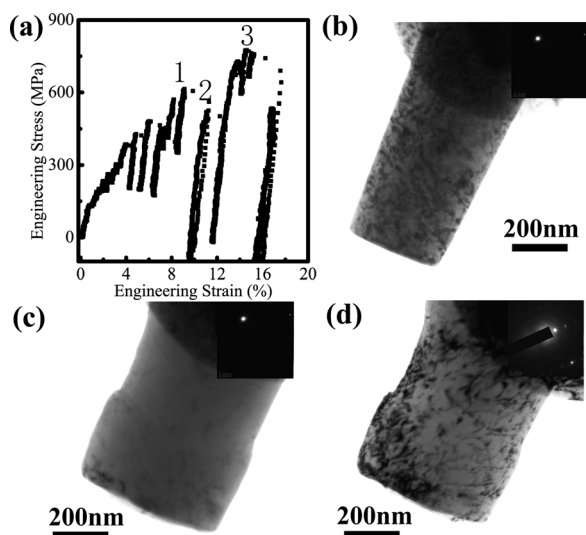


FIG. 2. Dislocations evolution in the Al pillar with $D = 430$ nm. (a) Engineering stress vs. engineering strain. (b) Bright-field image of the pillar before compression. (c) Bright-field image taken after the tests indicates that almost all the dislocations under present image condition escaped away. (d) An image taken in a different orientation, demonstrating that a high density of jammed dislocations remains in the pillar after collapse (enhanced online) [URL: <http://dx.doi.org/10.1063/1.3681582.2>].

consistent with the dislocation avalanche picture outlined by Csikor *et al.* in their DDD simulations.¹⁵ This dynamic process continued until the collapse with a large strain burst ($\sim 5\%$) marked by point 3 as shown in Fig. 2(a). Afterwards, there are no visible dislocations left in this particular imaging orientation (Fig. 2(c)), suggesting that almost all the dislocations on the slip planes that can be seen in this imaging condition moved collectively out of the pillar in an avalanche, also in accord with the simulation-predicted picture of dislocation unjamming preferentially in a particular set of slip planes.^{15,22} However, after titling the sample, jammed dislocations were found to remain on other slip planes, as shown in Fig. 2(d). Our *in situ* TEM monitoring is consistent with the partial destruction and reconstruction of a jammed dislocation network proposed by Csikor *et al.*¹⁵

The actual collapse stress is different from the nominal (engineering) stress in Figs. 1(a) and 2(a), and the true collapse stresses can be determined by dividing the load by the instantaneous contact area right before a strain burst. This is done in Fig. 3, for all the pillars and their strain bursts. Again, we see two regimes: for the smaller group A pillars, collapses occurred at higher stresses, suggesting explosive dislocation generation²³ with a dislocation “meteor shower” through the pillar. For the larger group B pillars, large bursts occurred at relative low stresses (several hundred MPa). One typical example is shown in the inset of Fig. 3.

To summarize, for larger submicron pillars, strain bursts occur at a relatively low stress level (several hundred MPa) and the simulation-predicted dislocation avalanche picture appears relevant, where reconstruction of jammed dislocation network is the key. For small nanopillars, in contrast, pre-existing dislocations are mechanically annealed and the jammed dislocation configurations are not formed during subsequent straining. In the absence of such jamming, dislocations run wild across the sample, leading to immediate and

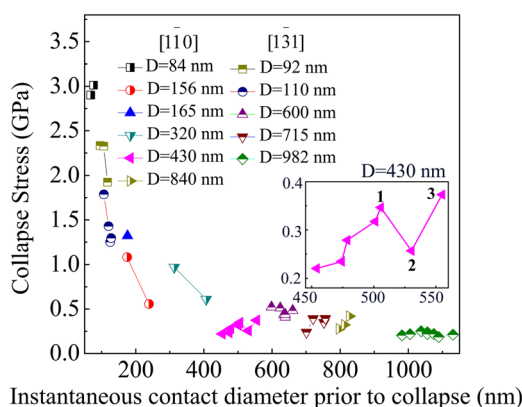


FIG. 3. (Color online) Collapse stress vs. the instantaneous contact diameter prior to the collapse (loading along $[220]$ and $[1\bar{3}1]$ direction, respectively). The inset is the magnified data for the $D = 430$ nm pillar showing the evolution of collapse stress vs. instantaneous contact diameter.

dramatic shape collapse while leaving the interior in an almost pristine state.

This work was supported by NSFC (50925104, 50831004, and 11131006) and 973 Programs of China (2010CB631003, 2012CB619402). We also appreciate the support from the 111 Project of China (B06025). J.L. acknowledges support by NSF CMMI-0728069, DMR-1008104 and DMR-1120901, and AFOSR FA9550-08-1-0325.

- ¹M. D. Uchic, D. M. Dimiduk, J. N. Florando, and W. D. Nix, *Science* **305**, 986 (2004).
- ²J. R. Greer and W. D. Nix, *Phys. Rev. B* **73**, 245410 (2006).
- ³C. A. Volkert and E. T. Lilleodden, *Philos. Mag.* **86**, 5567 (2006).
- ⁴S. W. Lee, S. M. Han, and W. D. Nix, *Acta Mater.* **57**, 4404 (2009).
- ⁵A. T. Jennings, M. J. Burek, and J. R. Greer, *Phys. Rev. Lett.* **104**, 135503 (2010).
- ⁶D. Kiener, W. Grosinger, G. Dehm, and R. Pippan, *Acta Mater.* **56**, 580 (2008).
- ⁷G. Richter, K. Hillerich, D. S. Gianola, R. Monig, O. Kraft, and C. A. Volkert, *Nano Lett.* **9**, 3048 (2009).
- ⁸C. P. Frick, B. G. Clark, S. Orso, A. S. Schneider, and E. Arzt, *Mater. Sci. Eng. A* **489**, 319 (2008).
- ⁹K. S. Ng and A. H. W. Ngan, *Acta Mater.* **56**, 1712 (2008).
- ¹⁰M. D. Uchic, P. A. Shade, and D. M. Dimiduk, *JOM* **61**, 36 (2009).
- ¹¹J. R. Greer and J. T. De Hosson, *Prog. Mater. Sci.* **56**, 654 (2011).
- ¹²W. D. Nix and S. W. Lee, *Philos. Mag.* **91**, 1084 (2011).
- ¹³T. A. Parthasarathy, S. I. Rao, D. M. Dimiduk, M. D. Uchic, and D. R. Trinkle, *Scr. Mater.* **56**, 313 (2007).
- ¹⁴S. I. Rao, D. M. Dimiduk, T. A. Parthasarathy, M. D. Uchic, M. Tang, and C. Woodward, *Acta Mater.* **56**, 3245 (2008).
- ¹⁵F. F. Csikor, C. Motz, D. Weygand, M. Zaiser, and S. Zapperi, *Science* **318**, 251 (2007).
- ¹⁶S. Brinckmann, J. Y. Kim, and J. R. Greer, *Phys. Rev. Lett.* **100**, 155502 (2008).
- ¹⁷D. M. Dimiduk, C. Woodward, R. LeSar, and M. D. Uchic, *Science* **312**, 1188 (2006).
- ¹⁸H. Bei, S. Shim, E. P. George, M. K. Miller, E. G. Herbert, and G. M. Pharr, *Scr. Mater.* **57**, 397 (2007).
- ¹⁹D. Mordehai, S. W. Lee, B. Backes, D. J. Srolovitz, W. D. Nix, and E. Rabkin, *Acta Mater.* **59**, 5202 (2011).
- ²⁰A. M. Minor, S. A. S. Asif, Z. W. Shan, E. A. Stach, E. Cyranowski, T. J. Wyrobek, and O. L. Warren, *Nature Mater.* **5**, 697 (2006).
- ²¹Z. W. Shan, R. K. Mishra, S. A. S. Asif, O. L. Warren, and A. M. Minor, *Nature Mater.* **7**, 115 (2008).
- ²²P. D. Ispanovity, I. Groma, G. Gyorgyi, F. F. Csikor, and D. Weygand, *Phys. Rev. Lett.* **105**, 085503 (2010).
- ²³E. Rabkin and D. J. Srolovitz, *Nano Lett.* **7**, 101 (2007).
- ²⁴See supplementary material at <http://dx.doi.org/10.1063/1.3681582> for movie S1, the movie/snapshot recorded during the compression of the $D = 165$ nm Al pillar inside TEM, and movie S2, the movie/snapshot recorded during the compression of the $D = 430$ nm Al pillar inside TEM.